

RTK signaling modulates the Dorsal gradient

Aharon Helman¹, Bomyi Lim², María José Andreu³, Yoosik Kim², Tatyana Shestkin¹, Hang Lu⁴, Gerardo Jiménez³, Stanislav Y. Shvartsman² and Ze'ev Paroush^{1,*}

SUMMARY

The dorsoventral (DV) axis of the *Drosophila* embryo is patterned by a nuclear gradient of the Rel family transcription factor, Dorsal (DI), that activates or represses numerous target genes in a region-specific manner. Here, we demonstrate that signaling by receptor tyrosine kinases (RTK) reduces nuclear levels and transcriptional activity of DI, both at the poles and in the mid-body of the embryo. These effects depend on *wntD*, which encodes a DI antagonist belonging to the Wingless/Wnt family of secreted factors. Specifically, we show that, via relief of Groucho- and Capicua-mediated repression, the Torso and EGFR RTK pathways induce expression of *WntD*, which in turn limits DI nuclear localization at the poles and along the DV axis. Furthermore, this RTK-dependent control of DI is important for restricting expression of its targets in both contexts. Thus, our results reveal a new mechanism of crosstalk, whereby RTK signals modulate the spatial distribution and activity of a developmental morphogen in vivo.

KEY WORDS: Dorsal, *Drosophila*, Gene regulation, Negative feedback, RTK signaling, *WntD*

INTRODUCTION

Dorsoventral (DV) patterning in the *Drosophila* embryo depends on the ventral-to-dorsal nuclear concentration gradient of Dorsal (DI) (Rogers and Schier, 2011). DI is a Rel family transcription factor that regulates the expression of over 50 target genes in a concentration-dependent manner (Reeves and Stathopoulos, 2009). Region-specific transcriptional control by nuclear DI subdivides the embryo into three germ layers: regions exposed to high, medium and low levels of nuclear DI ultimately give rise to mesoderm, neuroectoderm and dorsal ectoderm, respectively (Chopra and Levine, 2009; Stathopoulos and Levine, 2002).

DI is a bi-functional transcription factor that either activates or represses expression of its targets, depending on promoter context. It activates mesoderm-determining genes such as *twist* and *snail* (*sna*) (Ip et al., 1992; Jiang et al., 1991; Pan et al., 1991); yet, in the same nuclei it also represses, together with auxiliary proteins, the expression of dorsalizing genes such as *decapentaplegic* (*dpp*) and *zerknüllt* (*zen*) (Huang et al., 1993; Jiang et al., 1991). Notably, both modes of DI-dependent transcriptional regulation appear inactivated at the embryonic poles where, correspondingly, *sna* is not expressed and *dpp* and *zen* are transcribed.

Previous work has suggested that the Torso RTK pathway affects expression of DI targets at the termini (Casanova, 1991; Goldstein et al., 1999; Häder et al., 2000; Rusch and Levine, 1994). Torso-mediated signaling specifies terminal cell fates by locally activating mitogen-activated protein kinase/extracellular signal-regulated kinase (MAPK/Erk), which then phosphorylates and downregulates the general repressors Capicua (Cic) and Groucho (Gro) (Astigarraga et al., 2007; Cinnamon et al., 2008; Goff et al., 2001;

Häder et al., 2000; Jiménez et al., 2000; Liaw et al., 1995; Paroush et al., 1997). Cic and Gro have been implicated in repression of *zen* and *dpp* (Dubnicoff et al., 1997; Jiménez et al., 2000), providing a mechanism by which Torso controls DI targets. In addition, Torso signaling induces other genes such as *tailless* (*tl*) and *huckebein* (*hkb*) (Brönnner and Jäckle, 1991; Pignoni et al., 1990), and *Hkb* represses *sna* transcription at the termini (Reuter and Leptin, 1994; Goldstein et al., 1999). In both cases, the Torso pathway impinges on the transcriptional interpretation of the DI gradient.

Here, we demonstrate that the Torso pathway also modulates the DI gradient itself. We find that by downregulating Cic and Gro repression, Torso signaling induces expression of *wnt inhibitor of Dorsal* (*wntD*), a gene belonging to the Wingless/Wnt family and encoding a DI antagonist (Ganguly et al., 2005; Gordon et al., 2005). As *wntD* is also positively regulated by DI (Ganguly et al., 2005; Gordon et al., 2005; Zeitlinger et al., 2007), its expression occurs at the intersection between the domains of DI and activated MAPK/Erk, where it reduces the nuclear levels of DI. Using loss and gain-of-function assays, we show that Torso signaling acts as a gating mechanism that restricts expression of multiple DI target genes at the poles. Remarkably, a similar mechanism operates in the trunk region: DI and EGFR signaling induce *WntD*, which in turn downregulates DI and limits expression of its targets along the DV axis. In both contexts, inactivation of *wntD* results in altered expression patterns of multiple DI targets. Our results thus identify *wntD* as a crucial node for crosstalk between RTK signaling and the DI morphogen.

MATERIALS AND METHODS

Fly culture and stocks

Flies were cultured and crossed on yeast-cornmeal-molasses-malt extract-agar medium at 25°C. The following mutant alleles and Gal4 drivers were used: *wntD*^{KO1} (a kind gift from Mark McElwain and Raul Nusse, Stanford University, CA, USA), *Egfr*^{d2}, *rho*^{ve} *vn*¹, *nos-Gal4-VP16*, *UASp-Gro*^{AA} (Cinnamon et al., 2008; Helman et al., 2011), *Cic*^{ΔC2} (Astigarraga et al., 2007), *cic*¹, *trk*¹ and *tor*^{Y9}. Embryos lacking maternal *gro*, *ras* and *DSor* activities were derived from mosaic *gro*^{E48}, *ras*^{1e2f} and *DSor*^{LH110} (FlyBase) mutant germlines, respectively.

In situ hybridization and antibody staining

Embryos were dechorionated in bleach and fixed in 8% formaldehyde/PBS/heptane for 15–20 minutes. Expression patterns of *sog*, *lsc* and *wntD* were visualized by whole-mount in situ hybridization using

¹Department of Developmental Biology and Cancer Research, IMRIC, Faculty of Medicine, The Hebrew University, Jerusalem 91120, Israel. ²Department of Chemical and Biological Engineering and Lewis-Sigler Institute for Integrative Genomics, Princeton University, Princeton, NJ 08544, USA. ³Institut de Biologia Molecular de Barcelona-CSIC and Institut Catalana de Recerca i Estudis Avançats, Parc Científic de Barcelona, 08028-Barcelona, Spain. ⁴School of Chemical and Biomolecular Engineering and Parker H. Petit Institute for Bioengineering and Bioscience, Georgia Institute of Technology, Atlanta, GA 30332, USA.

*Author for correspondence (zparoush@cc.huji.ac.il)

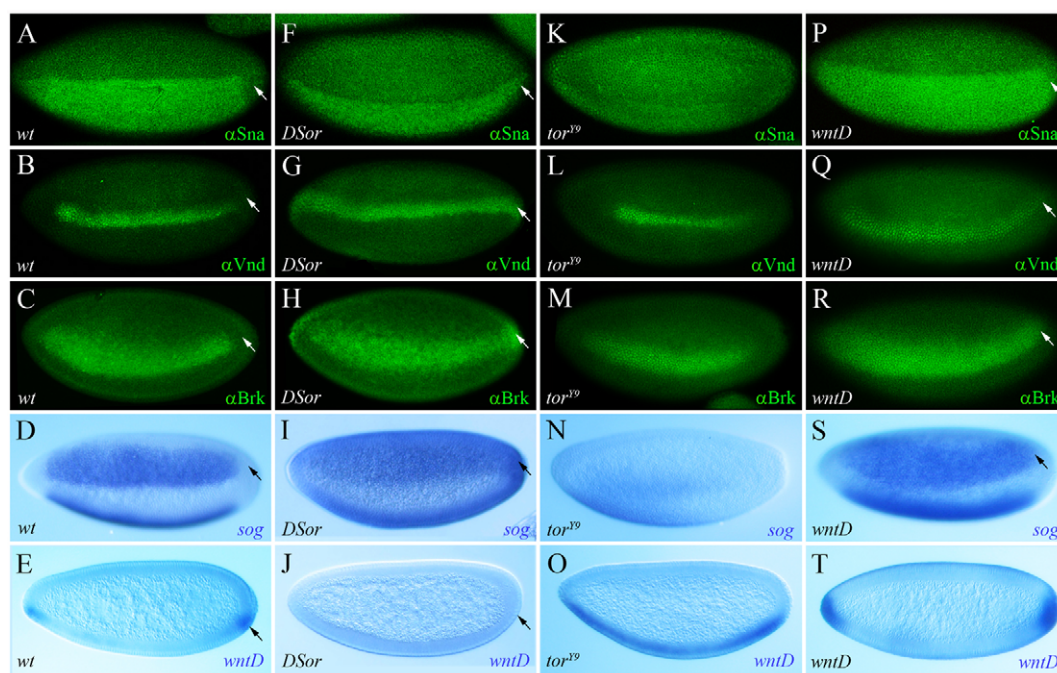


Fig. 1. Torso RTK signaling restricts expression of multiple Dorsal targets at the embryonic termini. (A–T) Lateral view of stage 5 wild-type (A–E), *DSor* (F–I), *tor^{Y9}* (K–O) and *wntD* (P–T) mutant embryos, immunostained for Sna (A,F,K,P), Vnd (B,G,L,Q) and Brk (C,H,M,R), or hybridized using digoxigenin-labeled RNA probes for *sog* (D,I,N,S) and *wntD* (E,J,O,T). Torso-dependent activity limits the expression of DI targets at the poles. (A–D) Expression of four DI targets, Sna, Vnd, Brk and *sog*, is confined to the trunk region and is excluded from the termini. (F–I) In *DSor* mutant embryos, where Torso signaling is blocked, expression of these DI targets expands into terminal regions. (K–N) In *tor^{Y9}* embryos, where Torso is overactive, expression of these DI targets retracts towards more central locations. (E,J,O) Torso signaling regulates *wntD* expression. Expression of *wntD*, normally observed in ventro-terminal positions (E), is lost in *DSor* mutants (J) and expands in *tor^{Y9}* embryos throughout the ventral region (O). (P–T) The DI targets Sna, Vnd, Brk, *sog* and *wntD* are ectopically expressed at the poles of *wntD* mutants, where DI is nuclear owing to the lack of functional WntD (see Fig. 2). Embryos are oriented with anterior to the left and dorsal side upwards. Arrows point to the posterior pole.

digoxigenin-UTP-labeled antisense RNA probes and anti-digoxigenin antibodies conjugated to alkaline phosphatase (Roche). Fluorescence in situ hybridization for *sna* and *vnd* was performed as described elsewhere (Kim et al., 2011).

Fluorescent immunodetection of activated MAPK/Erk in freshly fixed embryos (10% formaldehyde/PBS/Heptane buffer) was attained using rabbit α dpERK (1:100; Cell Signaling) (Helman and Paroush, 2010). Other antibodies used were: mouse α Dorsal (1:100; Developmental Studies Hybridoma Bank), rabbit α Ind (1:1000; kindly provided by Tonia von Ohlen, Kansas State University, USA), rat α Vnd (1:1000) (Helman et al., 2011), rat α Odd (1:200; Asian Distribution Center for Segmentation Antibodies, Mishima, Japan), rabbit α Lamin (1:500; kindly provided by Yosef Gruenbaum, The Hebrew University of Jerusalem, Israel), guinea pig α Brk and α Sna (1:500 and 1:200, respectively; kindly provided by Jessica Cande (IBDML, Marseille, France) and Mike Levine (UC Berkeley, USA) and sheep anti-DIG (1:200; Roche). Secondary antibodies were FITC- (1:2000), rhodamine- (1:2000) or Cy5-conjugated (1:800) (Jackson Laboratories). Embryos were mounted using DakoCytomation medium.

Microscopy and imaging

To minimize nonspecific effects caused by differential antibody or RNA probe concentrations and/or duration of staining reactions, wild-type control embryos expressing Histone-GFP (distinguishable by GFP expression) were mixed together with mutant embryos and simultaneously fixed and processed. Embryos were visualized, at $\times 20$ and $\times 40$ magnification, using a TE2000 inverted confocal laser scanning system (Nikon, Tokyo, Japan). Consecutive Z stakes were taken using a small aperture and converged to create a single image using EZ-C1 software (Nikon).

Imaging for quantification was performed on a Zeiss LSM510 confocal microscope. For lateral imaging of embryos, Zeiss 20 \times A-plan objective (NA=0.6) was used and images were obtained from a focal plane in the mid-sagittal plan cross section of an embryo. For end-on imaging, Zeiss 40 \times C-Apo water-immersion objective (NA=1.2) was used and images were collected from a focal plane ~ 75 μ m from either the anterior or posterior pole of an embryo.

To minimize variability brought about by the dynamics of the DI gradient, the distribution of nuclear DI and expression of its targets was quantified in embryos at late nuclear cycle 14, just before gastrulation. This stage was determined based on the appearance of ventrolateral dpERK staining and on the elongated, oval shape of nuclei (revealed by DAPI staining), both of which are observable ~ 30 minutes after the onset of cycle 14. Embryos doubly mutant for *rho* and *vn* do not stain for dpERK, and were therefore staged only by the shape of their nuclei.

Spatial gradients of nuclear DI and dpERK, or of *wntD* and *sna* mRNA, were extracted from confocal images of stained embryos using the previously described MATLAB image processing program (Kanodia et al., 2011). For imaging nuclear DI gradients, DAPI staining was used as a nuclear mask to indicate the position of nuclei. The mask was subsequently used to quantify the nuclear concentration of DI protein along the ventral-to-dorsal axis. For dpERK, *wntD* and *sna* expression profiles, cytoplasmic signals were also quantified.

For lateral imaging, images were pre-oriented so that the measurement starts from the mid-ventral point of an embryo. For end-on imaging, the raw nuclear DI gradient was fitted to a Gaussian curve and the fits were used to find the ventral-most position of the embryo, which corresponds to the maximum of the fit. For each embryo, two values of the nuclear DI gradient were extracted (from left and right of the ventral-most point, up to the dorsal side).

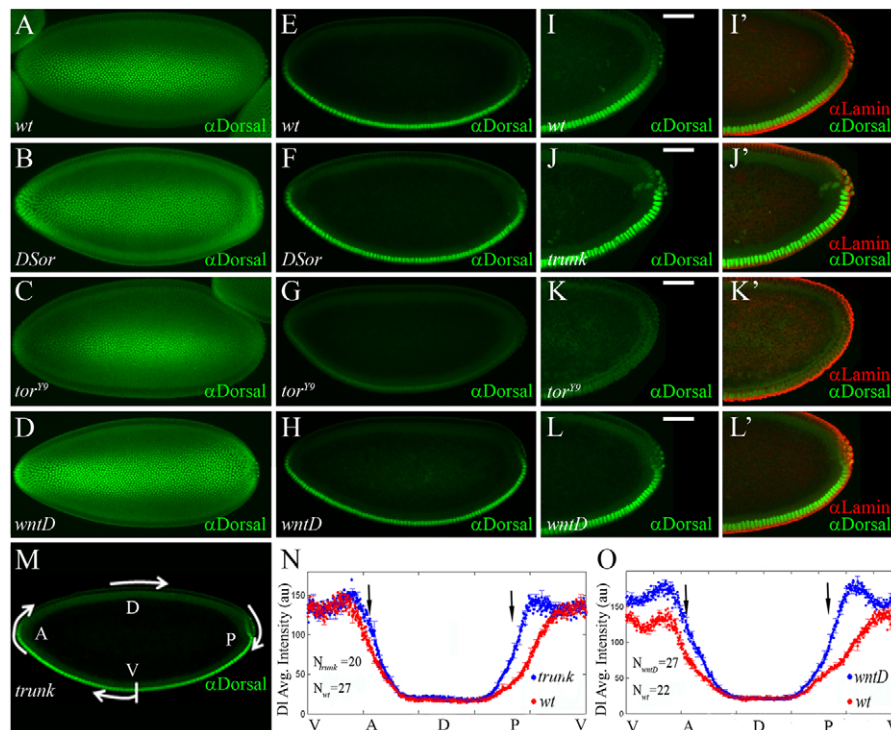


Fig. 2. The Torso pathway antagonizes nuclear localization of Dorsal. (A–M) Stage 5 embryos stained for DI (green). (A–D) Confocal z-stack images of ventral views, with anterior towards the left. (I–L) High magnification views of posterior poles of embryos stained for DI (green). (I'–L') Embryos were also co-stained for Lamin (red), showing that images truly correspond to sagittal cross-sections. Scale bars: 50 μ m. (A, E, I, I') Wild-type embryos. DI is nuclear on the ventral side and cytoplasmic dorsally. Note the declining nuclear DI accumulation towards the termini. (B, F) *DSor* mutants. (J, J') *trunk* mutants. DI is nuclear at the termini. (C, G, K, K') *tor*^{Y9} embryos. The domain of nuclear DI retracts towards the center of the embryo. (D, H, L, L') *wntD* mutants. DI is nuclear at the poles, as in *DSor* and *trunk* embryos. (M–O) Quantification of nuclear DI levels. (M) *trunk* mutant. The arrows indicate the clockwise, left-to-right direction of quantitative measurements of levels of nuclear DI, presented in the graphs. (E–M) Embryos are oriented with anterior to the left and dorsal side upwards. (N, O) Quantifying nuclear DI gradients in wild-type and mutant embryos. Solid line designates the average gradient; error bars indicate s.e.m. Levels of nuclear DI are significantly higher at the anterior and the posterior poles (black arrows) of *trunk* (N; blue line; $n=20$ embryos) and *wntD* (O; blue line; $n=27$ embryos) mutants, compared with wild-type embryos (red lines; $n=27$ and 22 embryos, respectively), suggesting that Torso-induced WntD antagonizes nuclear accumulation of DI at the termini.

RESULTS

Torso signaling excludes expression of multiple Dorsal target genes from the embryonic poles

As indicated above, previous studies had shown that expression of two DI target genes, *sna* and *zen*, is controlled by Torso signaling at the level of transcription. Correspondingly, the Sna protein is excluded from the termini of wild-type embryos (particularly from the posterior pole), but is detectable in the termini of *DSor* (*Drosophila* MEK) mutant embryos (Fig. 1A,F, respectively). To determine whether the Torso pathway influences DI-mediated transcriptional activity more broadly, we analyzed the expression profiles of multiple DI target genes in embryos lacking Ras/MAPK signaling activity. We find that additional primary DI targets, typically transcribed in the presumptive neuroectoderm, are ectopically expressed at the pole regions of *DSor* mutant embryos. One example is *ventral nervous system defective* (*vnd*), a gene normally activated by DI in two ventrolateral longitudinal stripes, one on either side, that extend along the trunk region of the embryo (Cowden and Levine, 2003; von Ohlen and Doe, 2000). The Vnd protein is never detected in terminal regions of wild-type embryos (Fig. 1B), but in the absence of MAPK/Erk activity it expands to the termini (Fig. 1G). Similarly, other DI targets, such as Brinker (Brk) and *short gastrulation* (*sog*), the expression of which is normally restricted to medial regions of the embryo at this stage

(Fig. 1C,D) (Markstein et al., 2004; Zhang et al., 2001), are detected throughout the anterior and posterior tips of *DSor* mutants (Fig. 1H,I).

To confirm that these effects result from loss of Torso pathway activity, we also analyzed expression of the DI target, Brk, in *trunk* mutant embryos, where Torso is never activated (Furriols et al., 1996). In this genetic background, Brk is expressed at the embryonic termini (supplementary material Fig. S1B). Conversely, the expression domains of Sna, Vnd, Brk and *sog* all retract to more central positions in *tor*^{Y9} embryos, where Torso is overactivated (Fig. 1K–N) (Halfar et al., 2001). These results support the idea that Torso signaling restricts expression of DI-regulated genes at the embryonic poles.

Torso signaling opposes nuclear localization of Dorsal at the termini

One possible explanation of the above results is that Torso signaling induces a transcriptional repressor that negatively regulates multiple DI-activated genes at the termini (see Discussion). However, Torso signaling might also act at the level of DI itself. To test the latter alternative, we compared the subcellular localization of DI in wild-type and mutant *DSor* or *tor*^{Y9} embryos. In stage 4 wild-type embryos, a gradient of nuclear DI forms along the DV axis (Chung et al., 2011; Kanodia et al., 2011),

but graded distribution of nuclear DI is also evident along the anteroposterior axis: DI is largely nuclear at the center of the embryo, but this accumulation declines towards the termini (Fig. 2A,E,I). We find that in *DSor* mutants, where Torso signaling is abolished, DI is nuclear even in terminal regions (Fig. 2B,F), an effect that is also observed in *trunk* mutants (Fig. 2J,M; see Fig. 2N and supplementary material Fig. S2A for quantification of nuclear DI in *trunk* versus wild-type embryos). Reciprocally, *tor^{Y9}* mutant embryos exhibit reduced levels of nuclear DI, even in ventro-central positions (Fig. 2C,G,K). Collectively, these results indicate that Ras/MAPK signaling negatively regulates nuclear levels of DI.

Torso signaling induces expression of the Dorsal feedback inhibitor *wntD*

How could the Torso pathway affect the nuclear localization of DI? Two reasons led us to consider the possibility that WntD, a novel member of the Wingless/Wnt family of secreted factors, links Torso signaling to DI. One, the *wntD* gene, known to be activated by DI, is transcribed in the ventral part of both embryonic poles at stage 4, when the Torso pathway is active (Fig. 1E) (Ganguly et al., 2005; Gordon et al., 2005; Zeitlinger et al., 2007); its expression, therefore, might also require a positive input by the Torso pathway. Two, *wntD* encodes an antagonist of DI nuclear localization, and could thus impinge on the expression of various DI targets (Ganguly et al., 2005; Gordon et al., 2005). We therefore hypothesized that *wntD* expression is induced by both Torso signaling and DI, and that subsequently WntD activity decreases nuclear DI at the termini.

To test this model, we triple stained wild-type embryos for *wntD* expression, nuclear DI and doubly phosphorylated MAPK/Erk (dpERK) that serves as readout for Torso signaling activity. This showed that *wntD* is expressed precisely where nuclear DI and dpERK intersect (Fig. 3A,A'). Furthermore, quantification of these images showed that, indeed, levels of *wntD* transcripts inversely correlate with levels of nuclear DI in ventral positions of both poles, consistent with downregulation of DI by WntD (Fig. 3B). We also found that *wntD* expression is absent at the termini of *DSor* and *trunk* mutant embryos (Fig. 1J and supplementary material Fig. S1D), whereas ectopic *wntD* transcription occurs along the ventral side of *tor^{Y9}* embryos, overlapping with the domain of nuclear DI (Fig. 1O and supplementary material Fig. S3). It is notable that these *wntD* responses are unique, given that expression of other positively regulated DI targets expands or retracts when Torso signaling is abrogated or overactivated, respectively (Fig. 1F-I,K-N).

Significantly, in *wntD* mutants the expression of multiple DI targets expands towards the termini (Fig. 1P-T and supplementary material Fig. S4), consistent with the accumulation of nuclear DI at this position (Fig. 2D,H,L; see Fig. 2O and supplementary material Fig. S2B for quantification of nuclear DI in *wntD* versus wild-type embryos). Thus, our data indicate that Torso signaling, acting via *wntD*, downregulates DI nuclear levels and expression of its targets at the embryonic poles. At the same time, these effects are milder than those observed in *DSor* and *trunk* mutants (Fig. 1F-I and supplementary material Fig. S1), suggesting the existence of additional mechanism(s) by which Torso negatively regulates DI targets (see Discussion).

EGFR signaling induces *wntD* expression and reshapes the gradient of nuclear Dorsal

Later in development, at stage 5/6, expression of *wntD* delineates the border between the presumptive mesoderm and neuroectoderm, where both DI and EGFR RTK activities converge (Fig. 3C,C')

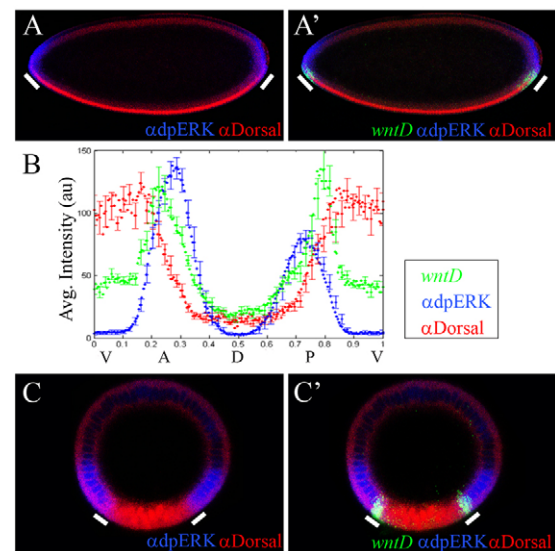


Fig. 3. *wntD* is expressed at the intersection of RTK signaling and Dorsal activity. (A-C') Wild-type embryos, triple stained for *wntD* transcripts (green), DI (red) and dpERK (blue). (A,A') Sagittal cross-sections of a stage 4 embryo. At this stage, dpERK staining reflects the activity of the Torso pathway. White bars indicate domains of *wntD* expression. (B) Quantification of *wntD* expression (green), nuclear DI (red) and dpERK (blue) in sagittal cross-sections of stage 4 wild-type embryos ($n=14$ embryos). Error bars indicate s.e.m. *wntD* is expressed at the junction of the two inputs and there is inverse correlation between the amounts of *wntD* and nuclear Dorsal. (C,C') Cross-section views of a stage 6 wild-type embryo. At this stage, dpERK staining reflects MAPK/Erk activation that is dependent on EGFR signaling. *wntD* is expressed at the point of intersection of the domains of nuclear DI and activated MAPK/Erk. (A,B) Embryos are oriented with anterior to the left and dorsal side upwards.

(Ganguly et al., 2005; Gordon et al., 2005). Here, too, we find that *wntD* expression is lost in either *DSor* or *Egfr* mutant embryos (Fig. 4A-C), as in *dl* mutants (Ganguly et al., 2005), indicating that *wntD* is activated by EGFR and DI in combination, and that both regulatory inputs are required. We therefore asked whether, similar to the Torso pathway, EGFR signaling also acts through WntD to influence the DI gradient. To this end, we quantified levels of nuclear DI in wild-type embryos, and in *wntD* and *rhomboid vein* mutants (*rho vn*; in this genetic background, EGFR ligands are absent and the pathway is inactive). To minimize the influence of dynamic changes in formation of the DI gradient, the distribution of DI was quantified specifically in stage 6 embryos at late nuclear cycle 14, right before gastrulation (see Materials and methods). Strikingly, we find that levels of nuclear DI are significantly higher in *wntD* and *rho vn* mutants than in wild-type embryos (Fig. 4D-F; quantification presented in Fig. 4G,H and supplementary material Fig. S2C,D).

Statistical significance of this result was established in two different ways. First, by fitting the gradients to the Gaussian profile, we determined that the amplitude of the nuclear DI gradient, in both of these mutant backgrounds, showed statistically significant increase relative to the amplitude of the wild-type gradient ($P<0.001$). Second, we performed a pair-wise comparison of nuclear DI levels between each of these mutant backgrounds and wild-type embryos at multiple points along the DV axis. Based on this analysis, we established that removal of

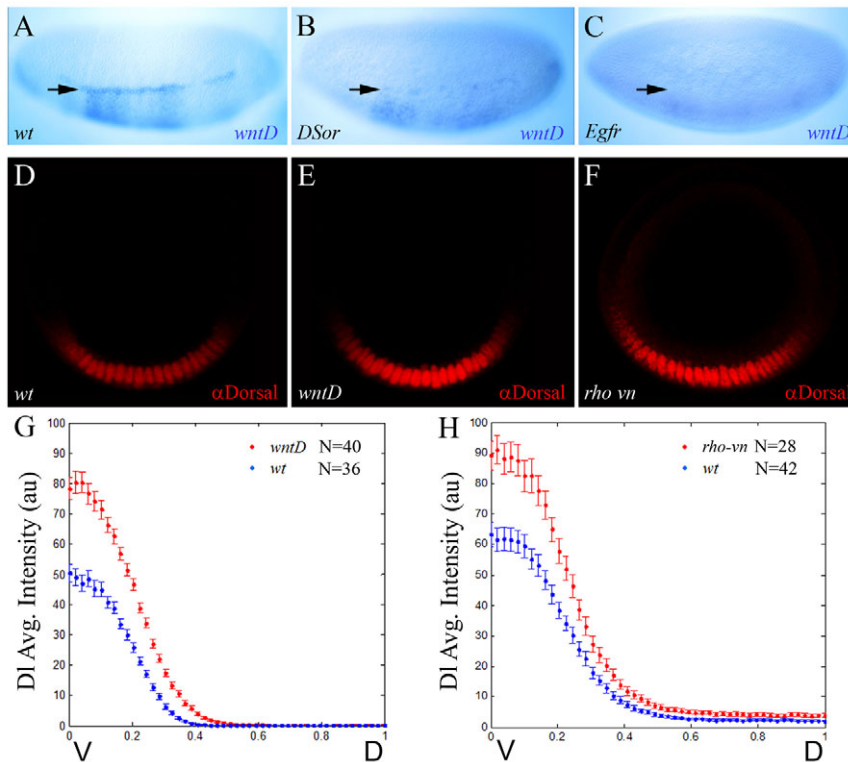


Fig. 4. The EGFR pathway induces *wntD* expression and limits the dorsoventral concentration gradient of nuclear Dorsal.

(A–C) Stage 6 wild-type (A) and mutant *DSor* (B) and *Egfr* (C) embryos were hybridized using a digoxigenin-labeled *wntD* RNA probe. RTK signaling is impeded in *DSor* (B) and *Egfr* (C) mutants, and the expression of *wntD* is blocked. The weak ventral *wntD* expression in the mutant embryos (B,C) probably results from ineffective induction by Df alone. Arrows point to the domain of *wntD* expression. (D–F) Representative cross-section images of stage 6 wild-type (D), *wntD* (E) and *rho vn* (F) embryos, stained for Df (red).

(A–C) Embryos are oriented with anterior to the left and dorsal side upwards. (G,H) Quantification of nuclear Df gradients along the DV axis in wild-type and mutant embryos. Data are the average gradients \pm s.e.m. Ventral levels of nuclear Df are significantly higher in *wntD* (G; red; $n=40$ measurements) and *rho vn* mutants (H; red; $n=28$ measurements), relative to wild-type controls (blue; $n=36$ and 42 measurements, respectively), suggesting that EGFR-induced WntD antagonizes nuclear accumulation of Df along the DV axis. For the nuclear Df gradient, two values were extracted from each embryo (see Materials and

wntD causes expanded nuclear accumulation of Df in at least the ventral 30% of the DV axis (supplementary material Fig. S5). Taken together, these results strongly indicate that the EGFR pathway induces *wntD* expression and in this way restricts Df nuclear localization along the DV axis.

WntD limits Dorsal target gene expression

To determine whether WntD-dependent regulation of nuclear Df affects DV patterning, we quantified the widths of expression domains for several Df targets in wild-type and mutant embryos (Fig. 5). Thus, we find that the *Sna* domain expands in stage 6 *wntD* and *DSor* mutants, relative to wild-type controls (Fig. 5D–F; note that the effect is more pronounced at the posterior of the embryo). Furthermore, quantification shows that the level of *sna* expression is significantly higher in *wntD* mutants, consistent with the increased levels of nuclear Df in this genetic background (Fig. 5A–C; supplementary material Fig. S2E). Similarly, the expression domains of two additional Df targets, Intermediate neuroblasts defective (*Ind*) and *lethal of scute* (*l'sc*), expand along the DV axis in *wntD* mutants (Fig. 5G–I; supplementary material Fig. S6). Noteworthy, *wntD* and wild-type embryos are of similar size, ruling out the possibility that these effects are simply due to size differences (supplementary material Fig. S7). We therefore conclude that *wntD* expression, under the control of EGFR signaling, plays an important role in regulating Df activity and, correspondingly, the expression of multiple Df targets along the DV axis.

Induction of *wntD* requires relief of Groucho- and Capicua-mediated repression

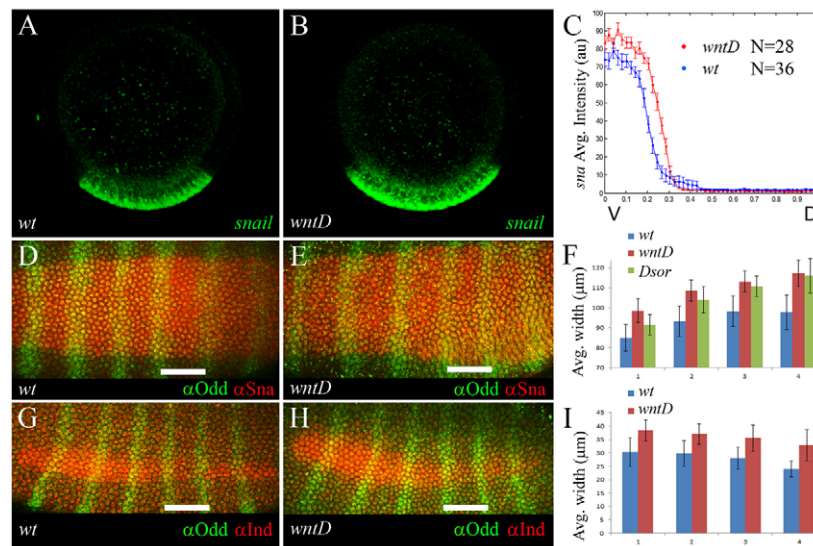
Our work shows that *wntD* is a novel target of the terminal system, which (together with Df) induces localized *wntD* expression. Activation of other known Torso pathway targets, such as *hkb* and *tll*, relies on relief of repression. Acting downstream of Torso,

MAPK/Erk phosphorylates and downregulates Cic and Gro, enabling localized induction of *tll* and *hkb* by broadly distributed activators. We find that, similarly, *wntD* is subject to repression by Cic and Gro, that is alleviated by the Torso pathway. Thus, *wntD* expression expands medially in embryos devoid of maternal *gro* or *cic*, albeit only in ventral positions where Df is nuclear (Fig. 6A–C). Accordingly, in both mutant backgrounds the levels of nuclear Df are significantly reduced (Fig. 6D–I), resembling the effects observed in *tor^{Y9}* embryos (Fig. 1O, Fig. 2C,G,K). Furthermore, the lower Df nuclear concentration in *gro* and *cic* embryos correlates with decreased Df target gene expression; for example, both mutant backgrounds exhibit attenuated Vnd expression in the lateral ectoderm (Fig. 6J–L).

In support of these results, we find that expression of unphosphorylatable variants of both Gro (*Gro^{AA}*) and Cic (*Cic^{AC2}*), which are insensitive to Torso-mediated downregulation (Astigarraga et al., 2007; Cinnamon et al., 2008; Hasson et al., 2005), reduce *wntD* mRNA levels (supplementary material Fig. S8). This effect is comparable with that caused by mutations in *DSor* and *trunk* (Fig. 1J; supplementary material Fig. S1D). Thus, blocking Gro and Cic downregulation mimics the effect caused by the loss of Torso signaling, indicating that *wntD* expression is induced through derepression.

DISCUSSION

Specification of body axes in all metazoans is initiated by a small number of inductive signals that must be integrated in time and space to control complex and unique patterns of gene expression. It is therefore of utmost importance to unravel the mechanisms underlying crosstalk between different signaling cues that concur during early development. Here, we have elucidated a novel signal integration mechanism that coordinates RTK signaling pathways with the Df nuclear gradient, and thus with terminal and DV patterning of the *Drosophila* embryo.



methods).

Fig. 5. WntD restricts the dorsoventral extent of Dorsal target expression. (A,B) Cross-sections of stage 6 wild-type (A) and *wntD* mutant (B) embryos, hybridized using a fluorescent *sna* RNA probe (green). (C) Expression levels of *sna* were quantified along the DV axis (wild-type in blue and *wntD* in red; $n=28$ and 36 measurements, respectively). Data are the average gradients \pm s.e.m. Two values were extracted from each embryo (see Materials and methods). (D,E,G,H) Stage 6 wild-type (D,G) and *wntD* mutant (E,H) embryos, stained for the DI targets Sna (red; D,E) or Ind (red; G,H), together with Odd-skipped (Odd; green; D,E,G,H). The DV extent of the Sna and Ind expression domains was measured along Odd stripes 1-4. Scale bars: $50\mu\text{m}$. (D) Embryos are oriented with anterior to the left. (F) The average width (μm) of Sna expression in wild-type, *wntD* and *DSor* embryos, along Odd stripes 1-4 (blue, red and green bars, respectively; $n=12$, 11 and 6 embryos, respectively). Error bars indicate s.d. (I) The average width (μm) of Ind expression in wild-type and *wntD* embryos, along Odd stripes 1-4 (blue and red, respectively; $n=10$ embryos for each genotype). Ind is not expressed in *DSor* mutants. Error bars indicate s.d.

Previous work had identified an input by Torso signaling into specific transcriptional effects of DI. Our results establish a general mechanism, which involves RTK-dependent control of the nuclear DI gradient itself, and thus affects a large group of DI targets. This regulatory input is based on RTK-dependent derepression of *wntD*, a DI target that encodes a feedback inhibitor of the DI gradient. Thus, DI activates *wntD* effectively only when accompanied by RTK signaling, enabling region-specific negative-feedback control of the nuclear DI gradient (Fig. 7). In the absence of RTK signaling, *wntD* is not expressed and the levels of nuclear DI are elevated. Consequently, DI target genes are ectopically expressed, both at the poles and along the DV axis (Figs 1, 5).

Torso RTK signaling depends on maternal cues and is independent of the DI gradient. Thus, it can be viewed as a gating signal that operates only at the embryonic poles, where it controls DI-dependent gene regulation. However, the activity of the EGFR RTK pathway later on in development crucially depends on DI, which induces the neuroectodermal expression of *rhomboid*, a gene encoding a serine protease required for processing of the EGFR ligand Spitz (Bang and Kintner, 2000). In this case, EGFR-dependent induction of WntD represents a negative feedback loop that reduces nuclear levels of DI laterally and, consequently, limits the expression of multiple DI targets along the DV axis (Fig. 7).

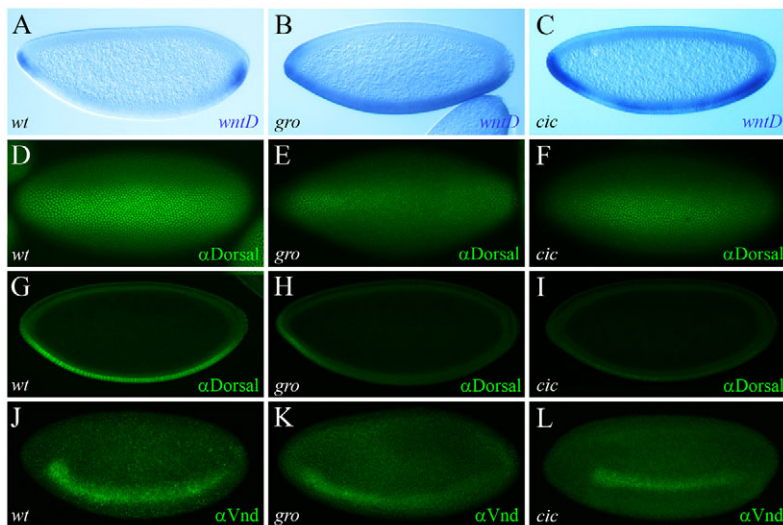


Fig. 6. RTK signaling promotes *wntD* expression via relief of Groucho- and Capicua-dependent repression. (A-C) Stage 4 wild-type (A), *gro* (B) and *cic* maternal mutant (C) embryos, hybridized using a digoxigenin-labeled *wntD* RNA probe. There is ventral expansion of *wntD* expression in the mutants. (D-I) Stage 5 wild-type (D,G), *gro* (E,H) and *cic* mutant (F,I) embryos stained for DI (green). The reduced accumulation of nuclear DI in the two mutant backgrounds is evident both in ventral views (E,F; compare with D) and in sagittal cross-sections (H,I; compare with G). (J-L) Stage 5 embryos stained for Vnd (green). Note the weaker expression in *gro* (K) and *cic* (L) mutant embryos, compared with wild-type control (J). Embryos are oriented with anterior to the left.

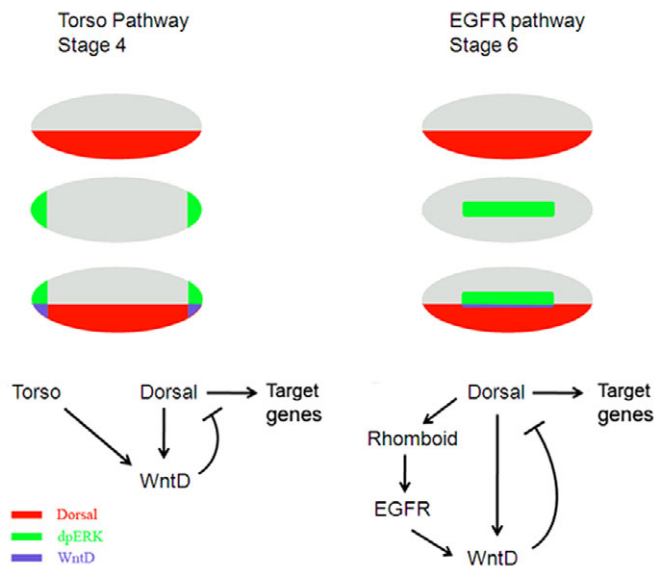


Fig. 7. Combinatorial induction of *wntD* expression by Dorsal and by RTK-mediated signaling. Nuclear DI (red) and RTK signaling (green) are both required for induction of *wntD* expression (blue). Accordingly, *wntD* is transcribed only where the domains of nuclear DI and activated MAPK/Erk converge, at the termini (stage 4; left) and in the neuroectoderm (stage 6; right). WntD antagonizes nuclear localization of DI, attenuating DI function as a transcriptional regulator. Early, at stage 4, the Torso pathway is activated independently of DI; hence, it acts, via *wntD*, as a gating mechanism that blocks DI-mediated activation and repression at the embryonic poles. Later on in development, at stage 6, DI-dependent EGFR pathway activity provides a negative-feedback regulatory mechanism that restricts DI target gene expression along the DV axis. Embryos are oriented with anterior to the left and dorsal side upwards.

It should be noted that the regulatory interactions that we have characterized do not preclude the existence of other mechanisms modulating nuclear DI concentration or activity. For example, the progressive dilution or degradation of maternal components involved in Toll receptor activation upstream of DI should cause reduced DI nuclear accumulation and retraction of its targets as development proceeds. It is also possible that Torso- or EGFR-induced repressors block transcription of DI target genes directly. Accordingly, the ectopic *sna* expression observed in embryos mutant for components of the Torso pathway such as *DSor* and *trunk* probably reflects both loss of WntD activity on DI and loss of Hkb-mediated repression of *sna*. In this context, it is interesting to note that *sna* expression expands and colocalizes with Hkb at the poles of *wntD* mutants (Fig. 1P) (Ganguly et al., 2005); perhaps repression of *sna* by Hkb is not sufficient to override increased DI activation in this genetic background. Thus, the Torso pathway probably employs more than one mechanism to exclude DI target expression from the termini. Furthermore, the existence of such additional regulatory mechanisms could explain why *wntD* mutants do not have a clear developmental phenotype, despite the broad effects on DI-dependent gene expression patterns caused by the genetic removal of *wntD* (this study) (Ganguly et al., 2005; Gordon et al., 2005). We propose that corrective mechanisms are present, which make the terminal and DV systems robust with respect to removal of the WntD-based feedback, such as RTK-induced repressors. Understanding the basis of this robustness will require additional studies.

Our work shows that RTK-dependent relief of Gro- and Cic-mediated repression is essential for transcriptional activation of *wntD* by DI. Correspondingly, in the absence of *cic* or *gro*, the early expression of *wntD* expands ventrally throughout the domain of nuclear DI. The early onset of this derepression, and the presence of at least one conserved Cic-binding site in the proximal upstream region of *wntD* (M.J.A. and G.J., unpublished), indicate that repression of *wntD* may be direct. Interestingly, it is thought that Gro and Cic are also involved in assisting DI-mediated repression of other targets such as *dpp* and *zen*, as *gro* and *cic* mutant embryos show derepression of those targets in ventral regions (Dubnicoff et al., 1997; Jiménez et al., 2000; Ratnaparkhi et al., 2006). However, as ectopic *wntD* expression in these mutants leads to reduced nuclear localization of DI along the ventral region, it is conceivable that decreased DI activity also contributes to the derepression of *dpp* and *zen*.

In conclusion, the data presented herein demonstrate RTK-dependent control of nuclear DI via *wntD*, based on multiple regulatory inputs, including negative gating, feed-forward loops and negative feedback control. Together, these mechanisms provide additional combinatorial tiers of spatiotemporal regulation to DI target gene expression. Future studies will show whether other signal transduction cascades and/or additional developmental cues also impinge on the DI morphogen gradient.

Acknowledgements

We thank Maayane Cohen, Rona Grossman, Adi Jacob and Sharon Mezuman for continued help and encouragement during this project. We are grateful to Benny Shilo for his comments on the manuscript and to Jessica Cande, Shari Carmon, Yosef Gruenbaum, Mike Levine, Mark McElwain, Raul Nusse, Benny Shilo, Tonia von Ohlen, the Developmental Studies Hybridoma Bank and the Bloomington Stock Center for antibodies, fly stocks and other reagents.

Funding

This research was supported by grants from the Israel Science Foundation (Center of Excellence; 180/09) and the Król Charitable Foundation to Z.P.; the National Institutes of Health [R01GM086537 from the National Institute of General Medical Sciences] to S.Y.S. and Z.P.; the National Science Foundation [1136913, EFRI-MIKS] to S.Y.S. and H.L.; and by ICREA, Ministerio de Ciencia e Innovación (BFU2008-01875) and Generalitat de Catalunya (2009SGR-1075) to G.J. A.H. was the recipient of a PhD Fellowship by the Rector of the Hebrew University. Deposited in PMC for release after 12 months.

Competing interests statement

The authors declare no competing financial interests.

Supplementary material

Supplementary material available online at <http://dev.biologists.org/lookup/suppl/doi:10.1242/dev.075812/-DC1>

References

- Astigarraga, S., Grossman, R., Díaz-Delfín, J., Caelles, C., Paroush, Z. and Jiménez, G. (2007). A MAPK docking site is critical for downregulation of Capicua by Torso and EGFR RTK signaling. *EMBO J.* **26**, 668-677.
- Bang, A. G. and Kintner, C. (2000). Rhomboid and Star facilitate presentation and processing of the *Drosophila* TGF- α homolog Spitz. *Genes Dev.* **14**, 177-186.
- Brönnér, G. and Jäckle, H. (1991). Control and function of terminal gap gene activity in the posterior pole region of the *Drosophila* embryo. *Mech. Dev.* **35**, 205-211.
- Casanova, J. (1991). Interaction between *torso* and *dorsal*, two elements of different transduction pathways in the *Drosophila* embryo. *Mech. Dev.* **36**, 41-45.
- Chopra, V. S. and Levine, M. (2009). Combinatorial patterning mechanisms in the *Drosophila* embryo. *Brief. Funct. Genomics Proteomics* **8**, 243-249.
- Chung, K., Kim, Y., Kanodia, J. S., Gong, E., Shvartsman, S. Y. and Lu, H. (2011). A microfluidic array for large-scale ordering and orientation of embryos. *Nat. Methods* **8**, 171-176.
- Cinnamon, E., Helman, A., Ben-Haroush Schyr, R., Orian, A., Jiménez, G. and Paroush, Z. (2008). Multiple RTK pathways downregulate Groucho-mediated repression in *Drosophila* embryogenesis. *Development* **135**, 829-837.

- Cowden, J. and Levine, M. (2003). Ventral dominance governs sequential patterns of gene expression across the dorsal-ventral axis of the neuroectoderm in the *Drosophila* embryo. *Dev. Biol.* **262**, 335-349.
- Dubnicoff, T., Valentine, S. A., Chen, G., Shi, T., Lengyel, J. A., Paroush, Z. and Courey, A. J. (1997). Conversion of Dorsal from an activator to a repressor by the global corepressor Groucho. *Genes Dev.* **11**, 2952-2957.
- Furriols, M., Sprenger, F. and Casanova, J. (1996). Variation in the number of activated *torso* receptors correlates with differential gene expression. *Development* **122**, 2313-2317.
- Ganguly, A., Jiang, J. and Ip, Y. T. (2005). *Drosophila* WntD is a target and an inhibitor of the Dorsal/Twist/Snail network in the gastrulating embryo. *Development* **132**, 3419-3429.
- Goff, D. J., Nilson, L. A. and Morisato, D. (2001). Establishment of dorsal-ventral polarity of the *Drosophila* egg requires *capicua* action in ovarian follicle cells. *Development* **128**, 4553-4562.
- Goldstein, R. E., Jiménez, G., Cook, O., Gur, D. and Paroush, Z. (1999). Hucklebein repressor activity in *Drosophila* terminal patterning is mediated by Groucho. *Development* **126**, 3747-3755.
- Gordon, M. D., Dionne, M. S., Schneider, D. S. and Nusse, R. (2005). WntD is a feedback inhibitor of Dorsal/NF-kappaB in *Drosophila* development and immunity. *Nature* **437**, 746-749.
- Häder, T., Wainwright, D., Shandala, T., Saint, R., Taubert, H., Brönnert, G. and Jäckle, H. (2000). Receptor tyrosine kinase signaling regulates different modes of Groucho-dependent control of Dorsal. *Curr. Biol.* **10**, 51-54.
- Halfar, K., Rommel, C., Stocker, H. and Hafen, E. (2001). Ras controls growth, survival and differentiation in the *Drosophila* eye by different thresholds of MAP kinase activity. *Development* **128**, 1687-1696.
- Hasson, P., Egoz, N., Winkler, C., Volohonsky, G., Jia, S., Dinur, T., Volk, T., Courey, A. J. and Paroush, Z. (2005). EGFR signaling attenuates Groucho-dependent repression to antagonize Notch transcriptional output. *Nat. Genet.* **37**, 101-105.
- Helman, A. and Paroush, Z. (2010). Detection of RTK pathway activation in *Drosophila* using anti-dpERK immunofluorescence staining. *Methods Mol. Biol.* **661**, 401-408.
- Helman, A., Cinnamon, E., Mezuman, S., Hayouka, Z., Von Ohlen, T., Orian, A., Jiménez, G. and Paroush, Z. (2011). Phosphorylation of Groucho mediates RTK feedback inhibition and prolonged pathway target gene expression. *Curr. Biol.* **21**, 1102-1110.
- Huang, J. D., Schwytter, D. H., Shirokawa, J. M. and Courey, A. J. (1993). The interplay between multiple enhancer and silencer elements defines the pattern of *decapentaplegic* expression. *Genes Dev.* **7**, 694-704.
- Ip, Y. T., Park, R. E., Kosman, D., Yazdanbakhsh, K. and Levine, M. (1992). *dorsal-twist* interactions establish *snail* expression in the presumptive mesoderm of the *Drosophila* embryo. *Genes Dev.* **6**, 1518-1530.
- Jiang, J., Kosman, D., Ip, Y. T. and Levine, M. (1991). The *dorsal* morphogen gradient regulates the mesoderm determinant *twist* in early *Drosophila* embryos. *Genes Dev.* **5**, 1881-1891.
- Jiménez, G., Guichet, A., Ephrussi, A. and Casanova, J. (2000). Relief of gene repression by *torso* RTK signaling: role of *capicua* in *Drosophila* terminal and dorsoventral patterning. *Genes Dev.* **14**, 224-231.
- Kanodia, J. S., Kim, Y., Tomer, R., Khan, Z., Chung, K., Storey, J. D., Lu, H., Keller, P. J. and Shvartsman, S. Y. (2011). A computational statistics approach for estimating the spatial range of morphogen gradients. *Development* **138**, 4867-4874.
- Kim, Y., Andreu, M. J., Lim, B., Chung, K., Terayama, M., Jiménez, G., Berg, C. A., Lu, H. and Shvartsman, S. Y. (2011). Gene regulation by MAPK substrate competition. *Dev. Cell* **20**, 880-887.
- Liaw, G. J., Rudolph, K. M., Huang, J. D., Dubnicoff, T., Courey, A. J. and Lengyel, J. A. (1995). The *torso* response element binds GAGA and NTF-1/Elf-1, and regulates *tailless* by relief of repression. *Genes Dev.* **9**, 3163-3176.
- Markstein, M., Zinzen, R., Markstein, P., Yee, K. P., Erives, A., Stathopoulos, A. and Levine, M. (2004). A regulatory code for neurogenic gene expression in the *Drosophila* embryo. *Development* **131**, 2387-2394.
- Pan, D. J., Huang, J. D. and Courey, A. J. (1991). Functional analysis of the *Drosophila twist* promoter reveals a *dorsal*-binding ventral activator region. *Genes Dev.* **5**, 1892-1901.
- Paroush, Z., Wainwright, S. M. and Ish-Horowitz, D. (1997). *Torso* signalling regulates terminal patterning in *Drosophila* by antagonising Groucho-mediated repression. *Development* **124**, 3827-3834.
- Pignoni, F., Baldarelli, R. M., Steingrimsson, E., Diaz, R. J., Patapoutian, A., Merriam, J. R. and Lengyel, J. A. (1990). The *Drosophila* gene *tailless* is expressed at the embryonic termini and is a member of the steroid receptor superfamily. *Cell* **62**, 151-163.
- Ratnaparkhi, G. S., Jia, S. and Courey, A. J. (2006). Uncoupling *dorsal*-mediated activation from *dorsal*-mediated repression in the *Drosophila* embryo. *Development* **133**, 4409-4414.
- Reeves, G. T. and Stathopoulos, A. (2009). Graded dorsal and differential gene regulation in the *Drosophila* embryo. *Cold Spring Harb. Perspect. Biol.* **1**, a000836.
- Reuter, R. and Leptin, M. (1994). Interacting functions of *snail*, *twist* and *huckebein* during the early development of germ layers in *Drosophila*. *Development* **120**, 1137-1150.
- Rogers, K. W. and Schier, A. F. (2011). Morphogen gradients: from generation to interpretation. *Annu. Rev. Cell Dev. Biol.* **27**, 377-407.
- Rusch, J. and Levine, M. (1994). Regulation of the *dorsal* morphogen by the *Toll* and *torso* signaling pathways: a receptor tyrosine kinase selectively masks transcriptional repression. *Genes Dev.* **8**, 1247-1257.
- Stathopoulos, A. and Levine, M. (2002). Dorsal gradient networks in the *Drosophila* embryo. *Dev. Biol.* **246**, 57-67.
- von Ohlen, T. and Doe, C. Q. (2000). Convergence of *dorsal*, *dpp*, and *egfr* signaling pathways subdivides the *drosophila* neuroectoderm into three dorsal-ventral columns. *Dev. Biol.* **224**, 362-372.
- Zeitlinger, J., Zinzen, R. P., Stark, A., Kellis, M., Zhang, H., Young, R. A. and Levine, M. (2007). Whole-genome ChIP-chip analysis of Dorsal, Twist, and Snail suggests integration of diverse patterning processes in the *Drosophila* embryo. *Genes Dev.* **21**, 385-390.
- Zhang, H., Levine, M. and Ashe, H. L. (2001). Brinker is a sequence-specific transcriptional repressor in the *Drosophila* embryo. *Genes Dev.* **15**, 261-266.